CTA200 Project

Isabella Armstrong
1006822967
isabella.armstrong@mail.utoronto.ca

May 15, 2023

1 Introduction

The existence of hypervelocity stars (HVS) provide unique insight into the structure of the Milky Way potential. Before studying how hows HVSs are impacted but subtle variations in the Milky Way potential, it is important to understand how they respond to non-subtle changes in the potential. This project uses `speedystar`([14], [9], [2], [4]) to propagate and perform photometry on mock HVS populations. Conservation of energy allows a relationship to be derived between the initial velocity, position, and galactic potential and the final velocity, position and potential of the HVS. By varying speedystar input parameters, the effects of the Milky Way halo mass on the HVS population is explored.

For this project, a script `CTA200Project.py` was written which uses `speedystar` to create an ejection catalog of HVSs (see 5 for installation instructions and trouble shooting). This catalog is then propagated through three different Milk Way potentials each with a different dark matter halo scale factor, creating three different star samples. A propagation.fits file is saved for each potential. A sub-sample of HVS with velocities greater than the escape velocity at their position is selected an photometry is performed, and a photometry.fits files is saved for each sample.

After generating the star samples and saving the necessary information, the .fits files containing the photometry information are read and the total Galactocentric position, velocities (GCv), and the Galactic escape velocity (Vesc) at the HVSs position are saved. Stars with absolute magnitude greater than 20.7 are selected. Plots of Distance vs HVS number and Vesc vs GCv are made and saved in both .pdf and .png formats.

2 Speedystar Structure

`speedystar` is a python program which generates mock catalogs of HVSs. It takes in an ejection model, which determines how the spatial and velocity distribution of the stars will be sampled. This project uses the Hills mechanism [7], implemented in `speedystar` as `speedystar.eject.Hills` ([14], [9]) to generate the catalog and saves the masses, velocities, ages, flight times, luminosity, radii and evolutionary stage of each star.

After the population is generated, a Galactic potential is defined and the star sample is propagated through the Galaxy in 0.1 Myr timesteps. This project uses the Galactic potential `speedystar.utils.mwpotential` [5], which allows us to vary the Milky Way halo mass.

After the sample is propagated, mock observations of the ejected stars are obtained. Apparent magnitudes in a variety of bands are saved. The dust map dust-map-3d.h5 is used when computing apparent magnitudes [1].

2.1 Milky Way Potential

As stated above, the function `speedystar.utils.mwpotential` is used to define a Galactic potential. This takes into account contributions from the Milky Way as well as the moving LMC potential. The potential is comprised of several sub components, whose values can be changed. The central massive black hole (MBH) is modeled by the Keplerian potential given in (1).

$$\Phi_{BH,GC}(r) = -G\frac{4 \times 10^6 M_\odot}{r} \tag{1}$$

where r is the Galactocentric distance. The Galactic Bulge is modeled by a Hernquist potential given by (2)[6] . This model was derived using the de Vaucouleurs profile, and its simple relation between density and potential make it easy to implement [3].

$$\Phi_{Bulge,GC}(r) = -\frac{GM_b}{r + r_b} \tag{2}$$

where $M_b = 3.4 \times 10^10 M_\odot$ and $r_b = 0.7$kpc [13]. The potential in the galactic disc is given by a Miyamoto-Nagai potential (3) [10].

$$\Phi_{Disc}(R, z) = -\frac{GM_d}{\sqrt{R^2 + (a_d + \sqrt{z^2 + b_d^2}}} \tag{3}$$

here $M_d = 10^{11} M_\odot$ is the disc mass, $a_d = 6.5$kpc is disc scale length and $b_d = 260$pc is disc scale height [13]. The values for M_b, r_b, M_d, a_d, and b_d were calculated by inferring the

Galactic potential with tidal streams and assuming that the dark matter halo is triaxial. [13]. The dark matter contribution is give by a spheroidal NFW potential [11].

$$\Phi_{NFW}(r) = -\frac{4\pi G\rho_0 R_s^3}{r}\ln\left(1+\frac{r}{R_s}\right) \tag{4}$$

and

$$\rho(x,y,z) = \frac{M_s}{4\pi r_s}\frac{1}{(\zeta/r_s)(1+\zeta/r_s)^2}, \zeta^2 = x^2+y^2+\frac{z^2}{c_{halo}} \tag{5}$$

where ρ_0 is some initial parameter that depends on the scale mass M_s. A scale radius of $R_s = 24.8$kpc is taken [15]. We assume a spherical dark matter halo and that $c_{halo} = 1$.

The LMC potenital is comprised of a Keplerian (1) plus Hernquist bulge (2). A LMC MBH mass of $10^5 M_\odot$ is assumed. The scale mass is taken as $M_{LMC} = 1.5 \times 10^{11} M_\odot$ and the scale radius is taken to be $R_{LMC} = 17.14$kpc [5]. The initial position of the LMC is take as its observed position and velocity today. The centre-of-mass position is $\alpha = 78.76°$, $\delta = -69.19°$ [17], propermotion of $(\mu_\alpha, \mu_\delta) = (1.91, 0.229)$mas/yr [8], heliocentric distance of 49.97 kpc [12], and radial velocity of +262.2 km/s [16] are used.

The total potential given by `speedystar.utils.mwpotential` is the sum individual potential components (6).

$$\Phi = \Phi_{BH,GC} + \Phi_{Bulge,GC} + \Phi_{disc} + \Phi_{NFW} + \Phi_{BH,LMC} + \Phi_{Bulge,LMC} \tag{6}$$

The default values for `speedystar.utils.mwpotential` are a NFW scale mass of $M_s = 0.76 \times 10^{12} M_\odot$, a radial profile $r_s = 24.8$kpc, an axis ration of $c = 1$, and the $T = True$ so that `triaxialNFWPotential` is used.

3 Conservation of Energy

HVSs are initial ejected with velocity v_1, at position r_1 where the strength of the Galactic potential is Φ_1. After propagation, they have velocity v_2, and position (r_2) where the strength of the potential is Φ_2. Since energy is conserved, a relationship between v_2 and the other parameters can be derived. The initial energy of an HVS is given by (7)

$$E_1 = \frac{1}{2}mv_1^2 + \Phi_1 \tag{7}$$

where m is the mass of the HVS. Energy conservation states that $E_1 = E_2$, where $E_2 = \frac{1}{2}mv_2^2 + \Phi_2$. Therefore

$$v_2^2 = v_1^2 + \frac{2}{m}(\Phi_1 - \Phi_2) \tag{8}$$

where Φ_1 and Φ_2 are 6 evaluated at r_1 and r_2 respectively.

4 Effects of Milky Way Halo Mass on HVS Properties

The value of the scale mass in the Milky Way dark matter halo effects the properties of the observable HVS sample. In order to explore these difference, a HVS ejection catalog was created. An ejection rate of 10^{-3} HVS/year was used. This is an order of magnitude larger than the default ejection rate of 10^{-4} HVs/year. This was done to improve statistics and better study the differences caused by varying the dark matter halo scale mass (M_s).

The HVS catalog was propagated through three different Milky Way potentials: $M_s = [0.076, 0.76, 1.76]$. A total of 5707 HVSs were propagated through the Milky Way potential. For a HVS to be detectable, its total Galactocentric velocity (GCv) must be greater than the escape velocity to infinity at the star's current position (Vesc). Additionally, it must have magnitude $\text{Gaia}_G < 20.7$ making it bright enough detect with the Gaia satellite. The number of these potentially detectable HVSs varied with M_s. For $M_s = 0.076$, 684 of the 5707 HVSs were detectable. For $M_s = 0.76$ this number was 538 and for $M_s = 1.76$ it was 433. Table (1) summarizes this information. As the mass of the Halo increases, so does the strength of the potential and as a result fewer of the HVS in the initial ejection catalog reach velocities greater than the escape velocity of the Galaxy after propagation.

Scale Mass (M_s)	# of Observable HVS	% of Ejection Catalog
0.076	684	12
0.76	538	9.4
1.76	433	7.6

Table 1: The number of observable HVSs and percentage of the original catalog that is observable for each scale mass.

The condition GCv > Vesc removed 20% of the initial ejection catalog for $M_s = 0.076$ up to 36% of the initial catalog for $M_s = 1.76$. As M_s increases so does the strength of the potential the ejection catalog is propagated through. Therefore it makes sense that the number of observable HVS decreases as the potential increases. The condition that $\text{Gaia}_G < 20.7$ removed an additional 85% to 88% of the remaining HVSs after the velocity condition was applied. Apparent magnitude is the greater limiting factor in observation. Unlike the velocity condition, there was only a 3% difference in the percentage that was removed for the different samples.

The total Galactocentric distance of the observable HVSs is shown in figure (1). Each HVS is assigned a number corresponding to its position in the initial ejection catalog. Different HVSs are observable depending on the value of M_s; however, the distribution in position for the three potentials is the same.

As discussed in section 3), the final velocity of an HVS depends on its initial velocity, position, and final position, and the strength of the Milky Way potential. Therefore, an HVS that is observable when propagated through the $M_s = 0.076$ potential may not have a great

enough velocity of escape the Galaxy when propagated through the $M_s = 1.76$ potential. This also accounts for why a larger percentage of the original ejection catalog is observable for $M_s = 0.076$ when compared to the greater scale factors.

As M_s increases, so does the escape velocity at a fixed Galactocentric velocity (GCv). Figure (2) plots GCv versus Vesc for the three simulations and clearly shows how increasing M_s corresponds to an increase in escape velocity. An increase in M_s corresponds to an increase in the strength of the Milky Way potential (see section 2.1 equations 4 and 5).

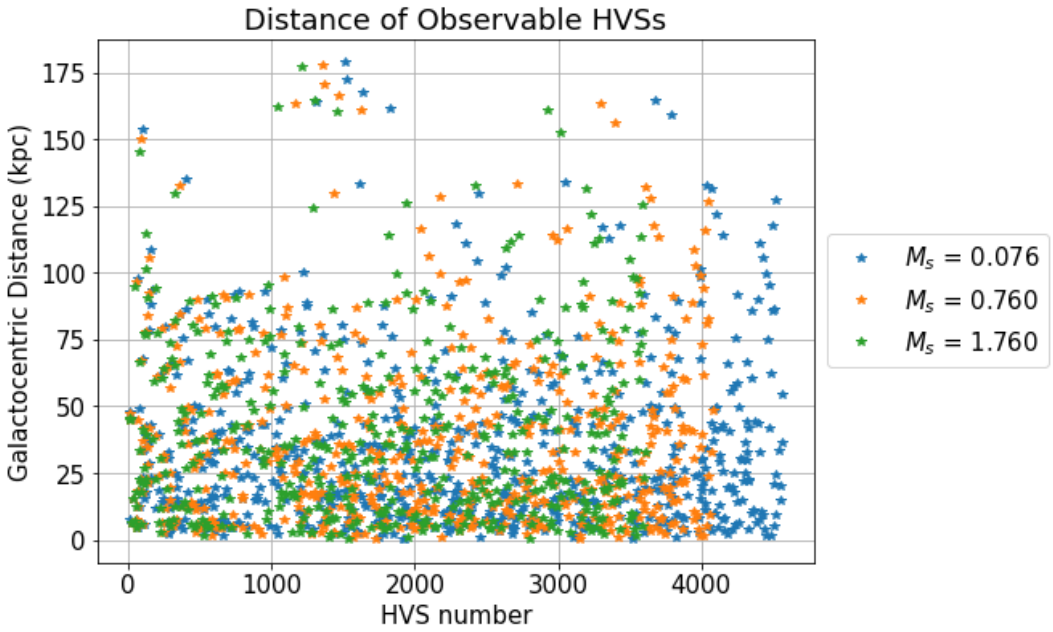

Figure 1: Galactocentric total distances in kpc of observable HVSs in the three simulations. After propagation, different HVSs are observable depending on the value of M_s. All three samples have the same distribution in GCv.

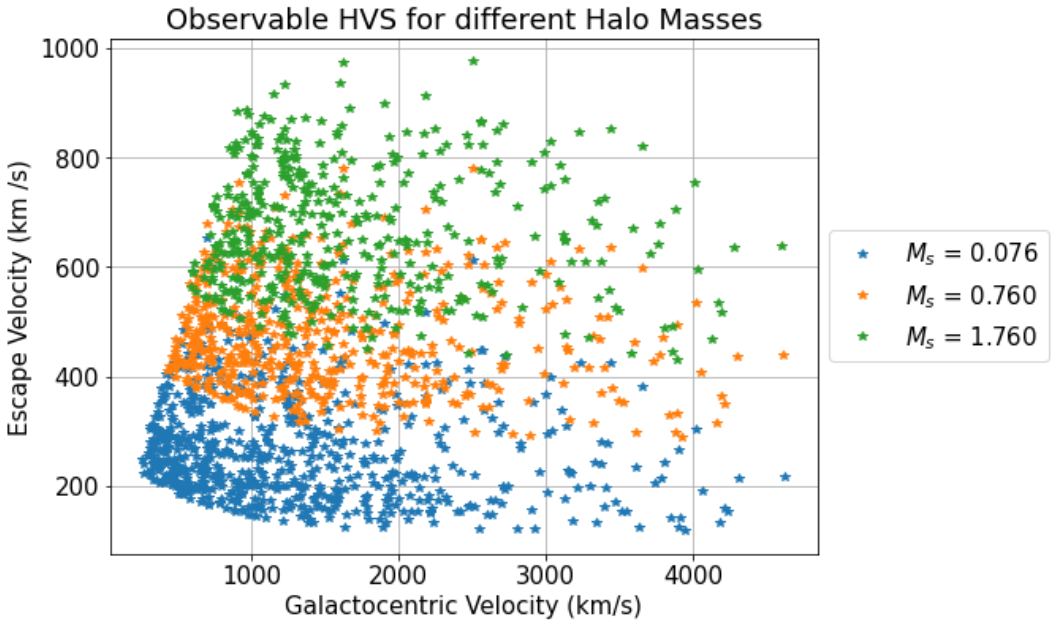

Figure 2: Escape Velocity versus total Galactocentric velocity for the three simulations. The blue stars correspond to the least massive halo with $M_s = 0.076$ and have lower escape velocities at a given GCv compared to the Green stars, corresponding to a scale mass of 1.76. The orange stars have $M_s = 0.76$; the default value.

5 Appendix

`speedystar` can be downloaded and installed from `https://github.com/fraserevans/speedystar`. Some trouble shooting notes

- In line 6 of setup.py there should be a comma after long_description
- pygaia has been uploaded since the last release of speedystar. Uninstall pygaia, and pip install pygaia==2.2. If this doesn't work, change line 88 from mysample.photometry() to mysample.photmetry(errors=None).
- the dust maps must be downloaded before running. Line 85 of my code calls on speedystar.fetch_dust(), which should download the dust maps for you. It didn't work on my installation but it should've. The dustmap I used can be directly downloaded from here `https://zenodo.org/record/31262/files/dust-map-3d.h5`
- A full Amuse installation is required. See `https://amuse.readthedocs.io/en/latest/install/howto-install-AMUSE.html#installing-amuse` for more detailed installation instructions if speedystar does not correctly install it the first time
- I initially had trouble with scanninglaw. My code doesn't use it so if a : No module named 'scanninglaw' asrise, you can comment out the line 12 in __init__.py and hopefully my code will run.

- Let me (or Fraser fraser.evans@utoronto.ca) know if any other issues arise.

References

[1] J. Bovy. Combined three-dimensional Milky Way extinction map, Sept. 2015.

[2] O. Contigiani, E. M. Rossi, and T. Marchetti. On measuring the Galactic dark matter halo with hypervelocity stars. *Monthly Notices of the Royal Astronomical Society*, 487(3):4025–4036, Aug. 2019.

[3] G. de Vaucouleurs. Recherches sur les Nebuleuses Extragalactiques. *Annales d'Astrophysique*, 11:247, Jan. 1948.

[4] F. A. Evans, T. Marchetti, and E. M. Rossi. Constraints on the Galactic Centre environment from Gaia hypervelocity stars II: The evolved population. *Monthly Notices of the Royal Astronomical Society*, 517(3):3469–3484, Dec. 2022.

[5] F. A. Evans, T. Marchetti, E. M. Rossi, J. F. W. Baggen, and S. Bloot. Comparing hypervelocity star populations from the large magellanic cloud and the milky way. *Monthly Notices of the Royal Astronomical Society*, 507(4):4997–5012, aug 2021.

[6] L. Hernquist. An Analytical Model for Spherical Galaxies and Bulges. *The Astrophysical Journal*, 356:359, June 1990.

[7] J. G. Hills. Hyper-velocity and tidal stars from binaries disrupted by a massive Galactic black hole. *Nature*, 331(6158):687–689, Feb. 1988.

[8] N. Kallivayalil, R. P. van der Marel, G. Besla, J. Anderson, and C. Alcock. Third-epoch Magellanic Cloud Proper Motions. I. Hubble Space Telescope/WFC3 Data and Orbit Implications. *The Astrophysical Journal*, 764(2):161, Feb. 2013.

[9] T. Marchetti, O. Contigiani, E. M. Rossi, J. G. Albert, A. G. A. Brown, and A. Sesana. Predicting the hypervelocity star population in Gaia. *Monthly Notices of the Royal Astronomical Society*, 476(4):4697–4712, June 2018.

[10] M. Miyamoto and R. Nagai. Three-dimensional models for the distribution of mass in galaxies. *Publications of the Astronomical Society of Japan*, 27:533–543, Jan. 1975.

[11] J. F. Navarro, C. S. Frenk, and S. D. M. White. The Structure of Cold Dark Matter Halos. *The Astrophysical Journal*, 462:563, May 1996.

[12] G. Pietrzyński, D. Graczyk, W. Gieren, I. B. Thompson, B. Pilecki, A. Udalski, I. Soszyński, S. Kozłowski, P. Konorski, K. Suchomska, G. Bono, P. G. P. Moroni, S. Villanova, N. Nardetto, F. Bresolin, R. P. Kudritzki, J. Storm, A. Gallenne, R. Smolec, D. Minniti, M. Kubiak, M. K. Szymański, R. Poleski, Ł. Wyrzykowski, K. Ulaczyk, P. Pietrukowicz, M. Górski, and P. Karczmarek. An eclipsing-binary distance to the Large Magellanic Cloud accurate to two per cent. *Nature*, 495(7439):76–79, Mar. 2013.

[13] A. M. Price-Whelan, D. W. Hogg, K. V. Johnston, and D. Hendel. Inferring the Gravitational Potential of the Milky Way with a Few Precisely Measured Stars. *The Astrophysical Journal*, 794(1):4, Oct. 2014.

[14] E. M. Rossi, T. Marchetti, M. Cacciato, M. Kuiack, and R. Sari. Joint constraints on the Galactic dark matter halo and Galactic Centre from hypervelocity stars. *Monthly Notices of the Royal Astronomical Society*, 467(2):1844–1856, May 2017.

[15] E. M. Rossi, T. Marchetti, M. Cacciato, M. Kuiack, and R. Sari. Joint constraints on the Galactic dark matter halo and Galactic Centre from hypervelocity stars. *Monthly Notices of the Royal Astronomical Society*, 467(2):1844–1856, 01 2017.

[16] R. P. van der Marel, D. R. Alves, E. Hardy, and N. B. Suntzeff. New Understanding of Large Magellanic Cloud Structure, Dynamics, and Orbit from Carbon Star Kinematics. *The Astronompical Journal*, 124(5):2639–2663, Nov. 2002.

[17] P. Zivick, N. Kallivayalil, G. Besla, S. T. Sohn, R. P. van der Marel, A. del Pino, S. T. Linden, T. K. Fritz, and J. Anderson. The Proper-motion Field along the Magellanic Bridge: A New Probe of the LMC-SMC Interaction. *The Astrophysical Journal*, 874(1):78, Mar. 2019.